



Enhanced reduction of bromate in water by 2-dimensional porous Co_3O_4 via catalytic hydrogenation

Duong Dinh Tuan^a, Hongta Yang^b, Nguyen Nhat Huy^c, Eilhann Kwon^d, Ta Cong Khiem^a, Siming You^e, Jechan Lee^{f,*}, Kun-Yi Andrew Lin^{a,*}

^a Department of Environmental Engineering & Innovation and Development Center of Sustainable Agriculture, National Chung Hsing University, 250 Kuo-Kuang Road, Taichung, Taiwan

^b Department of Chemical Engineering, National Chung Hsing University, 250 Kuo-Kuang Road, Taichung, Taiwan

^c Faculty of Environment and Natural Resources, Ho Chi Minh City University of Technology, VNU-HCM, 268 Ly Thuong Kiet St., Dist. 10, Ho Chi Minh City, Viet Nam

^d Department of Environment and Energy, Sejong University, 209 Neungdong-ro, Gunja-dong, Gwangjin-gu, Seoul, Republic of Korea

^e James Watt School of Engineering, University of Glasgow, Glasgow G12 8QQ, UK

^f Department of Environmental and Safety Engineering, Ajou University, Suwon 16499, Republic of Korea

ARTICLE INFO

Editor: Dr. Zhang Xiwang

Keywords:

Hydrogenation

Bromate

Bromide

H_2

Cobalt

Co_3O_4

ABSTRACT

As catalytic hydrogenation is validated as one of the most useful approach to reduce a potential carcinogenic bromate in water, the usage of continuous purge H_2 gas and precious metal catalysts are typically required, making it less feasible for practical implementation. Since sodium borohydride (NaBH_4) represents a potential alternative source for releasing H_2 and non-precious metal catalysts (cobalt (Co)) are usually required to accelerate the hydrolysis of NaBH_4 for faster H_2 production, the combination between Co-based catalysts and NaBH_4 could be favorable for bromate hydrogenation. Especially, it is even more advantageous to fabricate a porous heterogeneous catalyst with high surface area. Thus, this study aims to construct such a novel porous heterogeneous catalyst for reducing bromate using sodium borohydride. Herein, a Co-coordinated framework with TMC ligand (CoTMC) is employed as precursor, which is then transformed into hexagonal porous Co_3O_4 (HPCO) via one-step calcination. The resultant HPCO possesses remarkable surficial oxygen vacancies as well as textural properties in comparison with Co_3O_4 NP. Importantly, HPCO could completely reduce bromate to bromide within 20 min. The calculated bromate removal capacity using HPCO and NaBH_4 is achieved as 781.25 $\mu\text{mol/g}$, and the activation energy (E_a) is also calculated as 28.5 kJ/mol. Besides, HPCO also exhibits high catalytic activities for bromate reduction in the presence of various anions. Moreover, HPCO could be also reusable for reducing bromate to bromide over multiple-cycles without any remarkable change of catalytic activities. These features indicate that HPCO is a robust and effective heterogeneous catalyst for bromate reduction in water.

1. Introduction

Bromate anion (BrO_3^-), a typical bromine-based oxidation product, has been commonly found in different water systems [1,2]. Since bromate is regarded as a potential human carcinogenic compound, its maximum concentration has been regulated at 10 $\mu\text{g/L}$ by WHO and USEPA [3]. While the formation of bromate from ozonation process was reported previously [4], some recent studies also illustrated that bromate can be formulated via advanced oxidation processes (AOPs) [5,6]. Since AOPs have been extensively employed for wastewater treatments, it is critically urgent to remove bromate in water.

To date, there are numerous approaches for removing bromate including filtration [7], adsorption [8], biodegradation [9] and catalytic reduction [6,10–16]. Nevertheless, bromate is ineffectively removed via traditional techniques (e.g., filtration, adsorption or biodegradation) due to high-cost, long operation time and low bromate removal capacities. On the contrary, catalytic reduction stands out as a promising approach, in which bromate can be removed and converted expeditiously to bromide ions in the presence of reducing agents (e.g., H_2 gas) [10,12,16].

Recently, since the usage of continuous purge H_2 usually suffers from difficulties of low solubility, safety concerns and sophisticated storage,

* Corresponding authors.

E-mail addresses: jlee83@ajou.ac.kr (J. Lee), linky@nchu.edu.tw (K.-Y.A. Lin).

<https://doi.org/10.1016/j.jece.2021.105809>

Received 12 April 2021; Received in revised form 20 May 2021; Accepted 2 June 2021

Available online 5 June 2021

2213-3437/© 2021 Elsevier Ltd. All rights reserved.

chemical hydrides (e.g., NH_3BH_3 , LiBH_4 , NaBH_4), in particular, sodium borohydride (NaBH_4) receives increasing attention as a potential reductant to replace conventional H_2 gas to reduce bromate in water because NaBH_4 possesses high theoretical H_2 capacity (ca. 10.8 wt%), easy-handling and environmental friendliness [6,11,17–19]. Nevertheless, the self-decomposition of NaBH_4 in water for releasing H_2 gas is significantly low, making it inefficient to quickly reduce bromate ions. Thus, catalysts are usually required as an “activator” to facilitate H_2 released from NaBH_4 hydrolysis [20]. For instance, Nurbek and co-workers employed a Ni-based MOF for catalyzing NaBH_4 to reduce bromate to bromide [21]. Lin et al. prepared nanoscale cobalt/carbon nanocage (NCC) to facilitate hydrolysis of NaBH_4 to quickly release H_2 to convert bromate to bromide [6]. Another previous work also investigated MOFs as catalysts for accelerating NaBH_4 hydrolysis to reduce bromate in water [22].

Recently, precious metal catalysts have been investigated and exhibited high catalytic activities to bromate reduction [12,23,24]; however their expensiveness and scarcity restrict them for large-scale applications. In contrast, non-precious metal catalysts have been validated as potential alternatives implemented for removing bromate in water [6,11,12,21,25–27]. In particular, cobalt (Co) is proven as one of the most effective non-precious metal catalysts employed for catalyzing NaBH_4 hydrolysis and eliminating toxicants in water [6,25,28]. While homogeneous Co-based catalysts are commonly inconveniently employed for practical applications, heterogeneous Co-based catalysts, in particular, cobalt oxide (Co_3O_4) has been recently attracted increasing attention and extensively used for various catalytic applications [28–32]. Nonetheless, as bromate reduction is conducted in aqueous environment, Co_3O_4 nanoparticles (NPs) are easily accumulated in aqueous solution, hence losing its catalytic activities [33,34].

In this regard, immobilized/supported Co_3O_4 NP composites are validated as promising approaches to minimize aggregation issue [32, 35], however sophisticated procedure and long fabrication time are typically required, making it less feasible for practical applications. On the contrary, Co_3O_4 catalysts derived from Cobalt-based precursor could be another strategy, in which Co_3O_4 NP can be completely framed, therefore those NPs might be avoided from agglomeration [28,29]. More importantly, the fabricated Co_3O_4 catalyst could not only retain the morphology of the precursor but also consist of pores, enabling it become a porous Co_3O_4 catalyst [29,36]. This porous-structured Co_3O_4 catalyst should be advantageous for hydrolyzing NaBH_4 for H_2 production, then reducing bromate in water.

Herein, in this study, we proposed developing a robust and effective Co_3O_4 through a single step calcination of a Co-coordinated framework with TMC ligand (CoTMC), which was then employed for eliminating and reducing bromate in water. The resultant material not only retained the 2-dimensional (sheet-like) hexagonal morphology of CoTMC but also exhibited porosity, making it a hexagonal porous Co_3O_4 (HPCO). Unique characteristics of the as-prepared HPCO were analyzed by Scanning Electronic Microscopy (SEM), Transmission Electron Microscopy (TEM), X-ray powder diffraction (XRD), X-ray photoelectron spectroscopy (XPS), Raman spectroscopy. Besides, the effect of different parameters including catalyst and NaBH_4 concentrations, pH, temperature, co-existing anions using HPCO+ NaBH_4 for bromate reduction is also investigated. The reusability of HPCO was also evaluated and the catalytic reduction mechanism of bromate by HPCO+ NaBH_4 system was also interpreted.

2. Experimental

2.1. Materials

All chemicals reagents in this study were purchased from commercial suppliers and used as received without further purifications. Cobalt chloride (CoCl_2) (> 98%) was obtained from Choneye Pure Chemicals (Taiwan). Trismercaptoptriazine (TMC) ($\text{C}_3\text{H}_3\text{N}_3\text{S}_3$) (95%) was

purchased from Alfa Aesar (USA). Sodium borohydride (NaBH_4) (> 98%) was received from Acros Organics (USA). (Deionized (DI) water was prepared to less than 18 $\text{M}\Omega\text{-cm}$.

2.2. Preparation and characterization of HPCO

The fabrication procedure of HPCO was illustrated in Fig. 1(a). Firstly, the coordinated framework comprised of Co and TMC (CoTMC) was prepared by coordinating Co^{2+} ions with TMC ligand [37]. In brief, 0.015 mol of CoCl_2 was dissolved in 200 mL of DI water, followed by the addition of 0.017 mol of TMC. The mixture was then continuously stirred at ambient temperature for 1 h, then aged without stirring for 24 h. The precipitate was collected by centrifugation, washed thoroughly by DI water/ethanol and dried at 65 °C to afford CoTMC. Subsequently, CoTMC was calcined in air at 550 °C to result in HPCO.

Morphologies of HPCO were visualized using electronic microscopes (JEOL JSM-7800F and JEM-1400, Japan). The crystalline structure of HPCO was then analyzed by an X-ray diffractometer (Bruker, USA). The chemical composition was also determined by EDX spectroscopy (Oxford Instruments, UK). Moreover, the surface chemistry of HPCO was further examined by X-ray photoelectron spectroscopy (PHI 5000, ULVAC-PHI, Japan). The textural properties of HPCO were analyzed by a volumetric analyzer (Anton Paar ASIQ, Austria) to obtain the N_2 sorption isotherms. Temperature-programmed reduction (TPR) profiles of catalysts were determined by a chemisorption analyzer with a TCD detector (Anton Paar, ASIQ TPx, Austria). Raman spectroscopies of HPCO and commercial Co_3O_4 NP were determined using a Raman spectrometer (TII Nanofinder 30, Japan). Zeta potentials of HPCO were analyzed by a zetasizer (Malvern, UK).

2.3. Catalytic reduction of bromate

The catalytic activity of HPCO for bromate reduction was performed using batch experiments. In a typical experiment, a certain amount of HPCO (e.g., 100 mg/L) was added to 200 mL of bromate solution with the initial bromate concentration (C_0) was 10 mg/L (equivalent to 0.78 mM). At a certain reaction time t , a sample aliquot was withdrawn from the mixture and filtered by syringe filter (0.22 μm). Subsequently, the filtrate was analyzed using an ion chromatography system (Dionex ICS-1100, USA) to determine concentrations of residual bromate (C_t) and generated bromide (C_j) at a given time t . The bromate removal efficiency (q_t) of HPCO was calculated via the following formula (Eq. (1)):

$$q_t = \frac{(C_0 - C_t) \times V}{W} \quad (1)$$

where V is the solution volume and W is the mass of the catalyst. The generation capacity of bromide from reduction of bromate (q_j , $\mu\text{mol/g}$) at a certain reaction time was measured via the following formula (Eq. (2)):

$$q_j = \frac{(C_j - C_i) \times V}{W} \quad (2)$$

where C_j is the concentration of bromide detected in the solution at a certain time t ; and C_i is the initial concentration of bromide in the solution. The effect of different pH parameters (i.e., 3–11) was evaluated by adjusting the initial pH bromate solution using HCl (1 M) and NaOH (1 M). The effect of co-existing anions (e.g., nitrate, sulfate, phosphate) was examined by adding the equivalent concentration (i.e., 10 mg/L) to bromate solution. Recyclability of HPCO was performed by reusing recovered HPCO without any regeneration treatments.

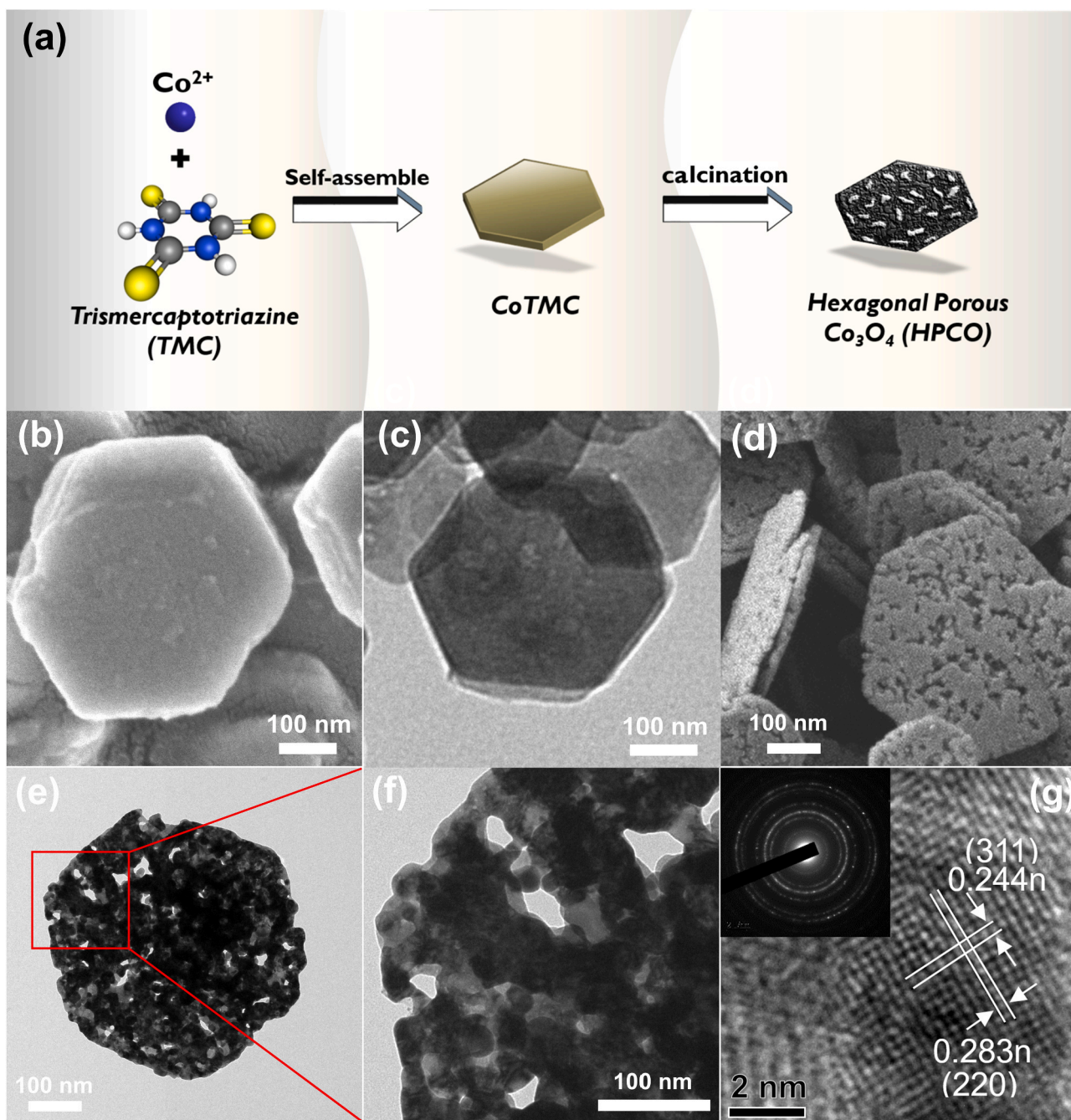


Fig. 1. (a) Schematic illustration for preparing HPCO; (b) SEM and (c) TEM images of CoTMC; (d) SEM and (e) TEM images of HPCO; and (f), (g) HRTEM images of HPCO (the inset is the SAED of HPCO).

3. Results and discussion

3.1. Characterizations of HPCO

Firstly, morphologies of the pristine precursor CoTMC were characterized to probe its appearance. Fig. 1 (b) and (c) presents SEM and TEM images of the as-fabricated CoTMC, showing that CoTMC possessed a hexagonal sheet-like morphology with smooth surfaces. After calcination processes, the resultant product still retained the hexagonal nanosheet-like morphology (shown in Fig. 1(d)) with the appearance of many pores. TEM image in Fig. 1(e) further reveals that those pores certainly existed and distributed throughout the substrate, confirming that the resultant calcined product was converted into a porous hexagonal nanosheet material. Moreover, Fig. 1(f) also reveals that this

calcined material was not only porous but also comprised of various spherical nanoparticles (NPs). The lattice-resolved HRTEM of this material showed two particular d -spacing values of 0.244 and 0.220 nm (Fig. 1(g)), which could be ascribed to the crystal plane of (311) and (220) of Co_3O_4 , respectively. This result confirms that the above-mentioned spherical NPs should be attributed to Co_3O_4 , demonstrating that CoTMC had been successfully transformed to Co_3O_4 after the calcination process, creating porous hexagonal nanosheet Co_3O_4 (HPCO). The inset of Fig. 1(g) provides the SAED of HPCO, illustrating a poly-crystalline structure of HPCO [38,39]. Besides, the size of those Co_3O_4 NPs HPCO was also determined in Fig. S1, confirming the nanoscale dimensions of these NPs.

The elemental analysis of HPCO was also determined using EDX spectroscopy as shown in Fig. 2(a) in which noticeable signals of Co and

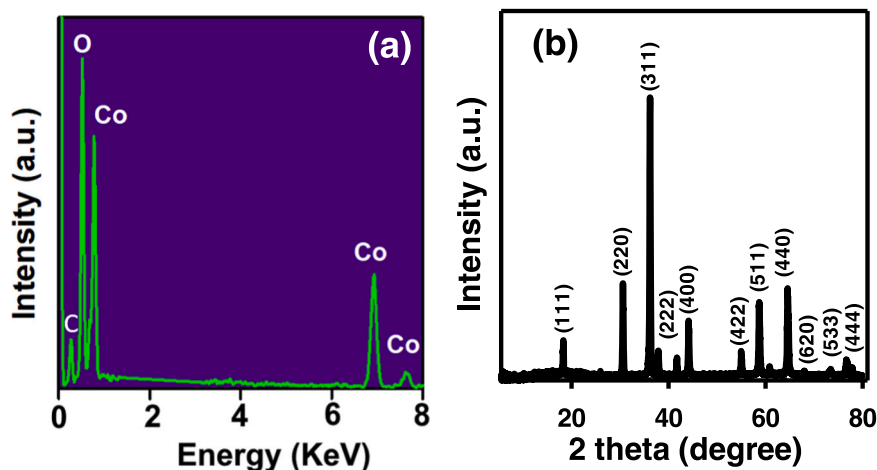


Fig. 2. Characterizations of HPCO: (a) EDX, and (b) XRD.

O were detected. A small peak at 0.3KeV could be ascribed to carbon (C), which possibly derived from carbon-coated layer on specimens. Besides, the crystalline structures of the pristine CoTMC and the resultant HPCO were further analyzed. Since the XRD patterns of CoTMC exhibited several noticeable peaks at 19, 32, 38, 51, 58, 61.6, 69.6 and 71.4° (Fig. S2), which were well-indexed to reported patterns [37], the

resulting HPCO showed totally different XRD patterns. Particularly, several diffraction peaks at 19.0°, 31.3°, 36.8°, 38.5°, 44.8°, 59.4° and 65.2° could be detected as shown in Fig. 2(b), which were corresponded to Co_3O_4 according to JCPDS #42-1467, further asserting the formation of Co_3O_4 of HPCO.

Additionally, an IR spectrum of HPCO was presented in Fig. 3(a).

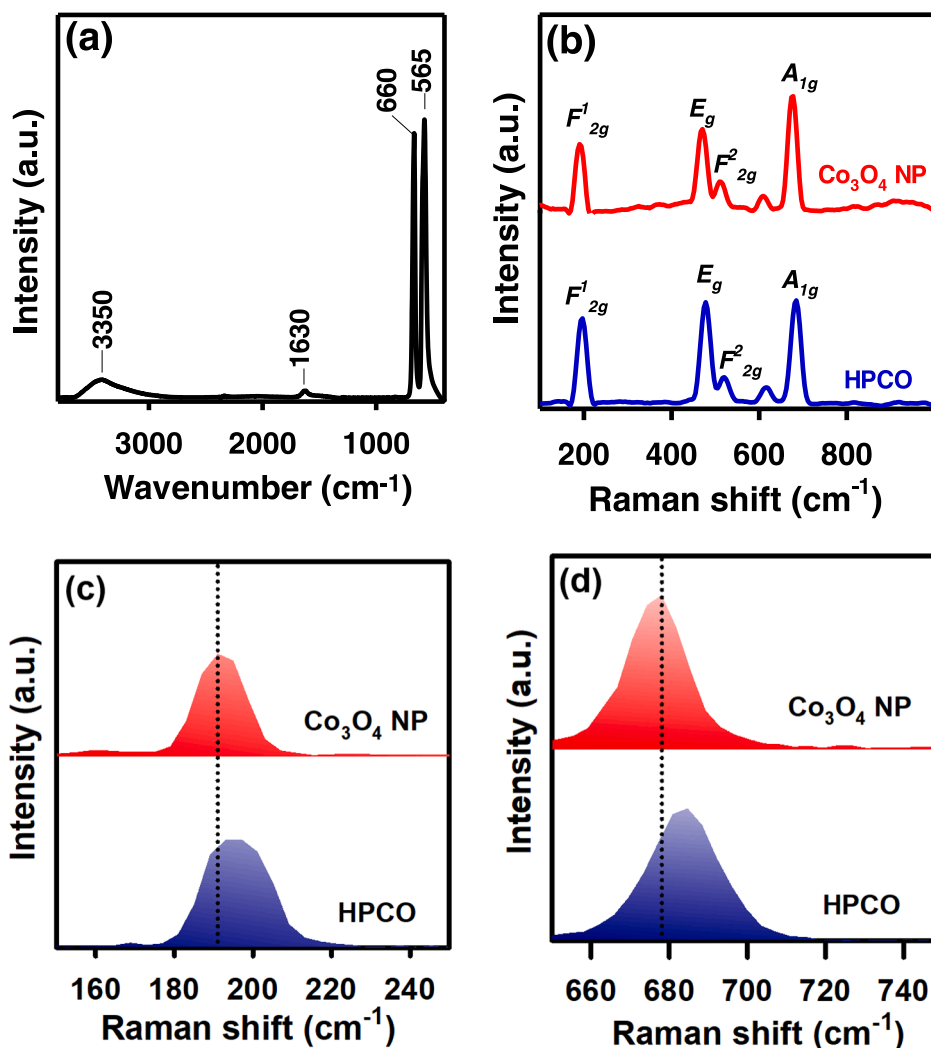


Fig. 3. Spectroscopies analyses of HPCO: (a) FTIR, (b) long-range Raman spectroscopy, (c) and (d) short-range Raman spectra at the regions of F_{2g}^1 and A_{1g} .

Two noticeable peaks could be observed at 565 and 660 cm^{-1} , corresponding to the stretching vibration modes of cobalt oxide for the tetrahedrally-bound Co^{2+} as well as octahedrally-bound Co^{3+} , respectively [40]. This result confirms the nature co-existence of Co^{2+} and Co^{3+} species in Co_3O_4 . Moreover, some small peaks were also detected at 1630 and 3350 cm^{-1} , attributed to the stretching and bending modes of (OH), which possibly derived from water molecules adsorbed on HPCO surfaces [41]. Furthermore, Raman spectroscopic analysis of HPCO was performed in Fig. 3(b), and some noticeable peaks could be found at 190, 472, 515 and 678 cm^{-1} , corresponded to F_{2g}^1 , Eg, F_{2g}^2 and A_{1g} modes of Co_3O_4 , respectively [42]. As Raman spectroscopy is commonly employed to verify oxygen vacancies of metal oxides, the reference catalyst, commercial Co_3O_4 NP, was also analyzed and compared with HPCO to probe differences of oxygen vacancies between HPCO and the commercial Co_3O_4 NP. As shown in Fig. 3(b), Raman spectrum of Co_3O_4 NP was comparable to that of HPCO, indicating that no obvious disordered structure of Co_3O_4 was present in HPCO [43]. Nevertheless, a closer spectra comparison between two materials at F_{2g}^1 and A_{1g} modes (displayed in Fig. 3(c) and (d)) reveals that these peaks had shifted. Particularly, the peak of F_{2g}^1 shifted from 190 to 193 cm^{-1} , while the peak of A_{1g} changed from 677 to 685 cm^{-1} . Since these peaks of F_{2g}^1 and A_{1g} were associated with $\text{Co}^{2+}\text{-O}^{2-}$, and $\text{Co}^{3+}\text{-O}^{2-}$, respectively [44,45], these shifting indicated that HPCO showed a higher degree of surficial oxygen vacancies than Co_3O_4 NP [46].

Furthermore, the surface chemistry of HPCO was also analyzed using XPS analysis. A full-survey spectrum of HPCO (Fig. S3) was determined, showing only Co and O species were detected. Fig. 4(a) also presents the Co2p spectrum of HPCO, which could be deconvoluted into multiple peaks. Particularly, the peaks at 779.2 and 794.1 eV could be corresponded to Co^{3+} species whereas the peaks at 780.6 and 795.8 eV could be ascribed to Co^{2+} species. These detected Co species further assures that the presence of Co_3O_4 in HPCO [47]. Besides, the O1s spectrum of HPCO was also analyzed as shown in Fig. 4(b), and two noticeable peaks at 529 and 531 eV could be attributed to metal-oxygen bond and R-O bond, respectively [48].

To further elucidate differences between HPCO and the commercial Co_3O_4 NPs, their redox characteristics were then determined by temperature-programmed reduction (TPR) measurements. Fig. 5(a) displays TPR profiles of HPCO and the commercial Co_3O_4 NP. The reduction process of HPCO started at a relatively low temperature at ca. 250 $^\circ\text{C}$, and a center temperature of the overall reduction profile occurred at 440 $^\circ\text{C}$, whereas the reduction process of Co_3O_4 NP started at 350 $^\circ\text{C}$ with a center temperature at 475 $^\circ\text{C}$. These comparisons indicated that while HPCO and the commercial Co_3O_4 NPs both

consisted of Co_3O_4 , their redox characteristics were noticeably different possibly owing to distinct surficial and morphological differences between these two catalysts.

In addition, textural properties of HPCO were also examined using N_2 sorption isotherms. As displayed in Fig. 5(b), the sorption isotherm of HPCO could be considered as an IUPAC type I isotherm, revealing that HPCO contained fine pores. The inset in Fig. 5(b) presented the pore size distribution, indicating that HPCO certainly comprised of mesopores, the corresponding specific surface area of HPCO was then measured as 13 m^2/g with a pore volume of 0.06 cm^3/g . For comparison, textural properties of a commercial Co_3O_4 NP were also characterized as shown in Fig. S4, and its specific surface area was determined as 2 m^2/g with a pore volume of 0.01 cm^3/g . This result demonstrates that HPCO possessed superior textural properties in comparison with that of Co_3O_4 NP, probably because Co_3O_4 NPs are easily agglomerated (as shown in Fig. S4)). On the contrary, though HPCO was also comprised of spherical Co_3O_4 NPs, these NPs could be refrained from agglomeration since Co_3O_4 NPs were framed into the 2D morphology.

Since catalytic reduction of bromate using HPCO catalyzed NaBH_4 is an aqueous-solution reaction, it was necessary to determine the surface charges of HPCO under different conditions using zeta potentials analysis as shown in Fig. 5(c). One can be seen that the surface charges of HPCO became more negative as the increase of pH. In particular, at pH = 3, the surface charge of HPCO was +31 mV, which was slightly reduced to +6 mV at pH = 5, then decreased to 0, -5 and -29 mV at pH = 7, 9 and 11, respectively. This result reveals that the surface charges of HPCO were positive under acidic conditions, then turned to negatively-charged under basic conditions with a $\text{pH}_{\text{zpc}} = \text{ca. } 7$.

3.2. Bromate reduction using HPCO with NaBH_4

Since bromate reduction was conducted in the presence of HPCO as an “activator” and NaBH_4 as a source for releasing H_2 , the reduction of bromate was firstly measured using individual constituent. Fig. 6(a) shows that bromate was negligibly reduced in the presence of HPCO alone, demonstrating that HPCO itself was incapable of removing bromate. When NaBH_4 was individually used to reduce bromate (without addition of catalysts), the concentration of bromate was barely decreased as C_t/C_0 was only 0.94, indicating that NaBH_4 alone could not reduce bromate efficiently, either. Nevertheless, when HPCO and NaBH_4 were simultaneously present, bromate was quickly reduced as C_t/C_0 reached nearly zero after 20 min, illustrating the effectiveness of HPCO catalyzed NaBH_4 to reduce bromate in water. The residual bromate concentration remained in the solution after reduction process was only

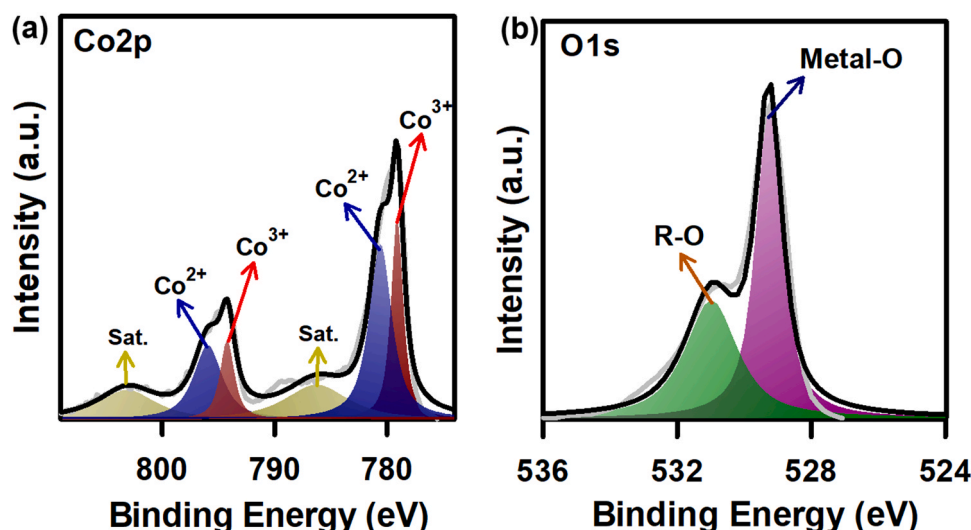


Fig. 4. XPS analysis of HPCO: (a) Co2p, and (b) O1s core-level spectra.

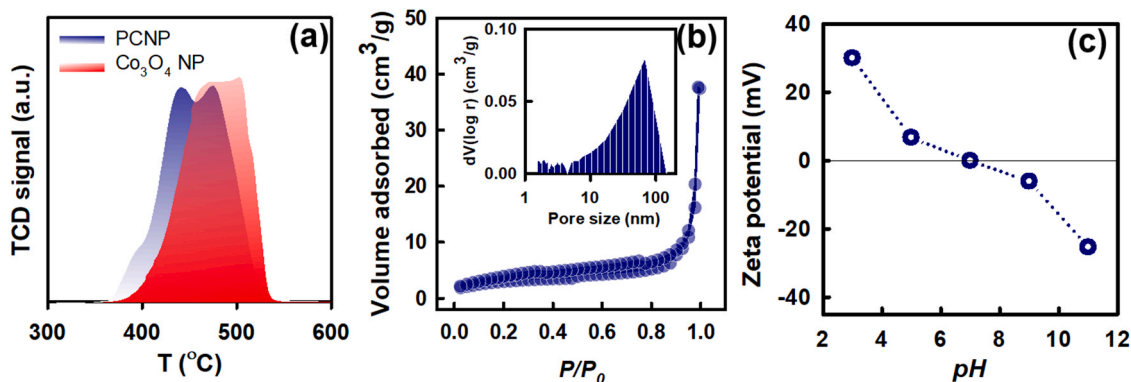


Fig. 5. Properties of HPCO: (a) TPR profile, (b) N_2 sorption isotherm and pore size distribution, and (c) zeta potentials.

0.03 $\mu\text{g/L}$, which is below the maximum bromate concentration in drinking water (i.e., 0.078 $\mu\text{g/L}$) regulated by WHO and USEPA. On the other hand, as HPCO was comprised of Co_3O_4 NP, the commercial Co_3O_4 NP was also employed as a reference catalyst for bromate reduction. As shown in Fig. 6(a), bromate was gradually reduced using commercial Co_3O_4 NP with C_t/C_0 only reached 0.79 after 60 min, which was much higher than that of HPCO. This result further confirms the superior catalytic activities of HPCO to bromate reduction in comparison with commercial Co_3O_4 NP.

Nevertheless, since the term of C_t/C_0 did not signify the amount of bromate reduced; therefore, bromate removal efficiencies per gram of catalyst ($\mu\text{mol/g}$) were necessarily determined as shown in Fig. 6(b). There was a small fraction of bromate (i.e., 44.7 $\mu\text{mol/g}$) was removed in the presence of sole NaBH_4 after 60 min, proving that without the addition of catalyst, bromate was inefficiently reduced. Besides, while bromate removal efficiencies (q_t) at 60 min of CoTMC and commercial Co_3O_4 NP were 101.6 and 163.9 $\mu\text{mol/g}$, respectively, HPCO exhibited a much higher bromate removal efficiency as q_t could reach nearly 781.25 $\mu\text{mol/g}$, an equilibrium, which is even higher than other reported catalysts in literature (shown in Table S1). This result further confirms that HPCO is an advantageous and promising heterogeneous catalyst for reducing bromate in water.

On the other hand, it was also crucial to determine whether bromate could be converted to bromide by those above-mentioned materials. As displayed in Fig. 6(c), almost no bromide generated after 60 min using sole NaBH_4 . When CoTMC and the commercial Co_3O_4 NP were employed, bromide generation capacities (q_f) were certainly detected, revealing that bromate was surely reduced to bromide. Moreover, as HPCO exhibited outstanding catalytic activities to bromate elimination, the corresponding generated bromide was also significantly higher than other materials, asserting the superior catalytic activity of HPCO for reducing and converting bromate to bromide. One can be noted that the generated bromide capacities were typically comparable to the amount of bromate reduced, suggesting that bromate was predominantly converted to bromide, and there was nearly no adsorption of removed bromate ions or produced bromide ions onto HPCO surface (Fig. S5).

As hydrolysis of NaBH_4 for releasing H_2 can be expedited in the presence of metal catalysts as follows (Eq. (3)) [49,50]:



the reaction of NaBH_4 with HPCO would produce H_2 which might then react with bromate to become bromide and H_2O as follows (Eq. (4)):



Fig. 6(d) shows H_2 evolution by NaBH_4 in the presence of HPCO, and H_2 evolution proceeded rapidly along with the reaction time, approaching an equilibrium after 20 min. The tendency of H_2 evolution was similar to that of bromate reduction in Fig. 6(a), suggesting that

removal of bromate by HPCO+ NaBH_4 would correlate to the reaction expressed in Eq. (4), which could take place via multiple potential mechanisms [12]. Firstly, H_2 would be evolved from HPCO-catalyzed hydrolysis of NaBH_4 , and the resulting H_2 would react with bromate ions in the bulk phase to transform bromate to bromide as illustrated in Fig. 6(e) as the route (i). On the other hand, bromate might temporarily reside on the surface of HPCO, and contact with H_2 molecules derived from HPCO-catalyzed NaBH_4 to become bromide as the route (ii) in Fig. 6(e).

Besides, as HPCO contained Co^{2+} , Co^{2+} would donate electrons to bromate and transform it to bromide while Co^{2+} was oxidized to Co^{3+} as the route (iii) in Fig. 6(e). Thus, XPS spectroscopy of used HPCO was analyzed as shown in Fig. S6; and the peak intensities of Co^{2+} and Co^{3+} were obviously changed compared to the pristine HPCO. This result validated that the oxidation of Co^{2+} to Co^{3+} certainly happened, which was then contributed to the reduction of bromate as illustrated in route (iii) of Fig. 6(e). Pandey et al. employed $\text{Ti}_3\text{C}_2\text{T}_x$ (MXene) for removing bromate and reported that the oxidation of Ti^{2+} to Ti^{4+} provided electrons to reduce bromate to bromide [51]. Another work by Restivo and co-workers also found that the reduction of bromate was certainly happened on the surface of metal catalyst in the presence of hydrogen atom in which metal was oxidized while bromate was contemporary reduced into bromide [12].

3.3. Effect of catalyst and NaBH_4 dosages

Since catalyst and NaBH_4 dosages are two crucial components to bromate reduction, the effect of HPCO dosage was first examined as displayed in Fig. 7(a–c). As discussed above, bromate was inefficiently removed in the absence of catalyst. Nevertheless, since a small amount of HPCO was adopted (i.e., 50 mg/L), the concentration of bromate was certainly reduced as C_t/C_0 was nearly 0.4 after 60 min with the corresponding removed bromate capacity was 1359.7 $\mu\text{mol/g}$. When HPCO dosage was increased to 100 mg/L, the concentration of bromate was quickly decreased as C_t/C_0 reached to nearly zero, and q_t was slightly reduced as 781.2 $\mu\text{mol/g}$. Further increase of HPCO dosage from 150 to 200 mg/L resulted in faster bromate reduction as C_t/C_0 could reach nearly zero in a shorter time with the corresponding q_t were 520.8 and 390.5 mg/L, respectively. These results reveal that though higher dosages of HPCO were more beneficial for reducing bromate, the removal efficiencies were decreased correspondingly. This is possibly because a higher dosage of catalyst did not fully contribute to the reduction of bromate in water, which is similar to reported literatures [14,52]. Moreover, one can be noted that bromide generation capacities were still comparable to reduced bromate concentrations, demonstrating that there were almost no adsorptions of bromate/bromide ions onto HPCO even at a higher dosage of HPCO.

In addition to catalyst dosage, since the presence of NaBH_4 as H_2 source is another important parameter for reducing bromate, it is also

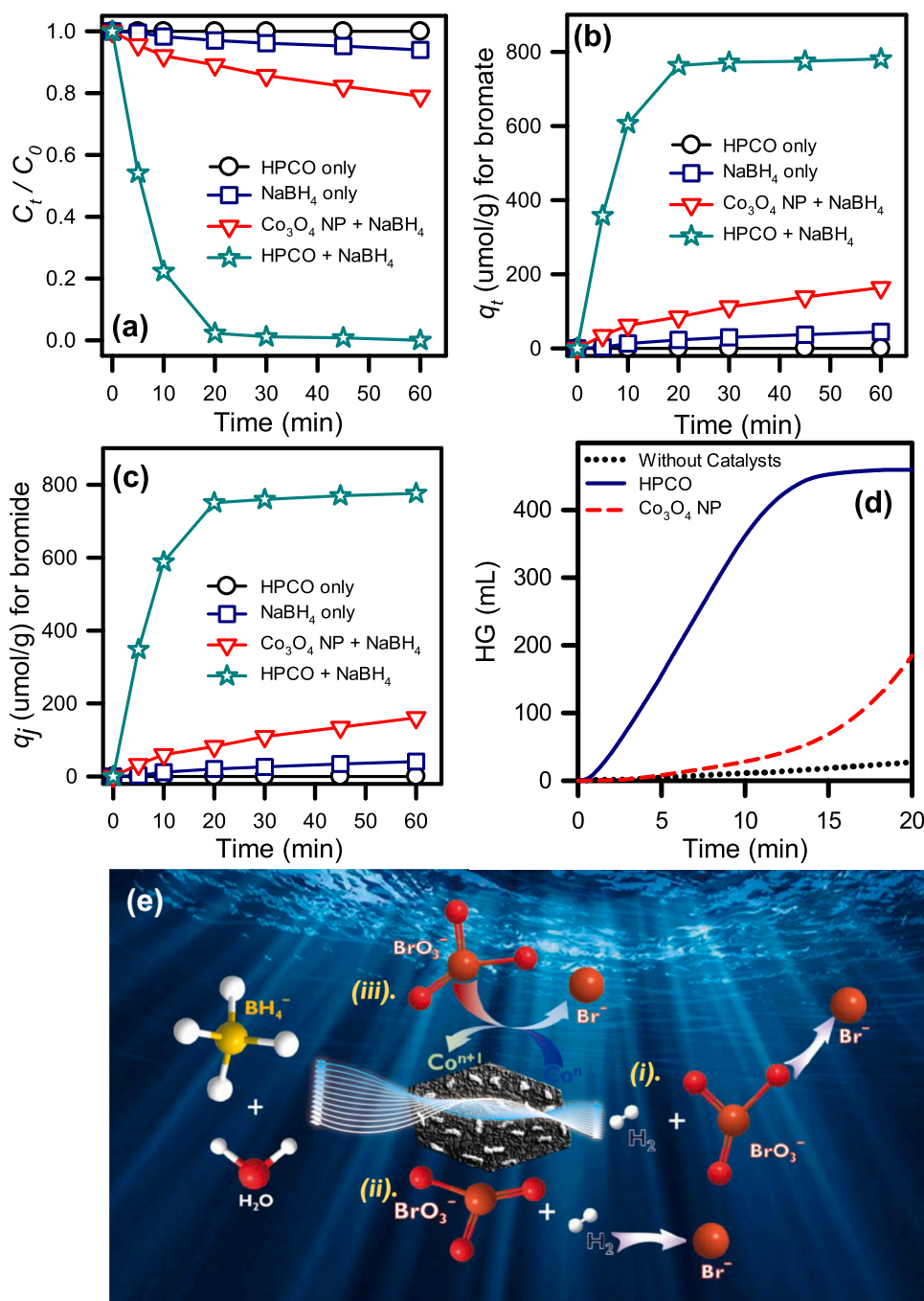


Fig. 6. Comparisons between HPCO only, NaBH₄ only, Co₃O₄ NP+NaBH₄ and HPCO+NaBH₄ for (a) bromate removal in terms of C_t/C_0 , (b) removal efficiency for bromate, (c) conversion efficiency of bromide (catalyst = 100 mg/L, NaBH₄ = 100 mg/L, T = 30 °C); (d) H₂ generation (T = 30 °C, catalyst = 500 mg/L, and NaBH₄ = 125 mM); and (e) the mechanisms of bromate reduction by HPCO+NaBH₄.

important to evaluate the variation of NaBH₄ dosage using HPCO as displayed in Fig. 7(d–f). At NaBH₄ = 50 mg/L, the concentration of bromate was gradually reduced as C_t/C_0 was 0.42 at 60 min, indicating that the reduction of bromate was insignificant in the lack of HG released from NaBH₄. Since NaBH₄ dosage was increased to 100 mg/L, bromate was rapidly reduced and fully removed within 20 min as C_t/C_0 reached nearly zero. Moreover, further increase of 125 mg/L of NaBH₄ enabled even faster bromate reduction within a certain shorter time. This finding suggests that a certain NaBH₄ dosage (i.e., 100 mg/L) is needed to afford completely bromate elimination by HPCO catalyzed NaBH₄ system. Similar results were also reported in literatures that bromate could be totally eliminated/reduced at a fixed amount of

NaBH₄ [6]. For further experiments, 100 mg/L of NaBH₄ is particularly selected to investigate other parameters.

3.4. Effect of temperatures

Temperature is also a critical factor for bromate reduction in water; therefore, the effect of different temperatures varying from 30 °C to 40 °C to bromate reduction using HPCO catalyzed NaBH₄ was further examined. As displayed in Fig. 8, bromate was totally eliminated/reduced within 20 min at 30 °C, which was even faster in shorter time at higher temperatures. In particular, 100% of bromate was achieved in 15 min at 35 °C whereas all bromate was reduced within 10 min at

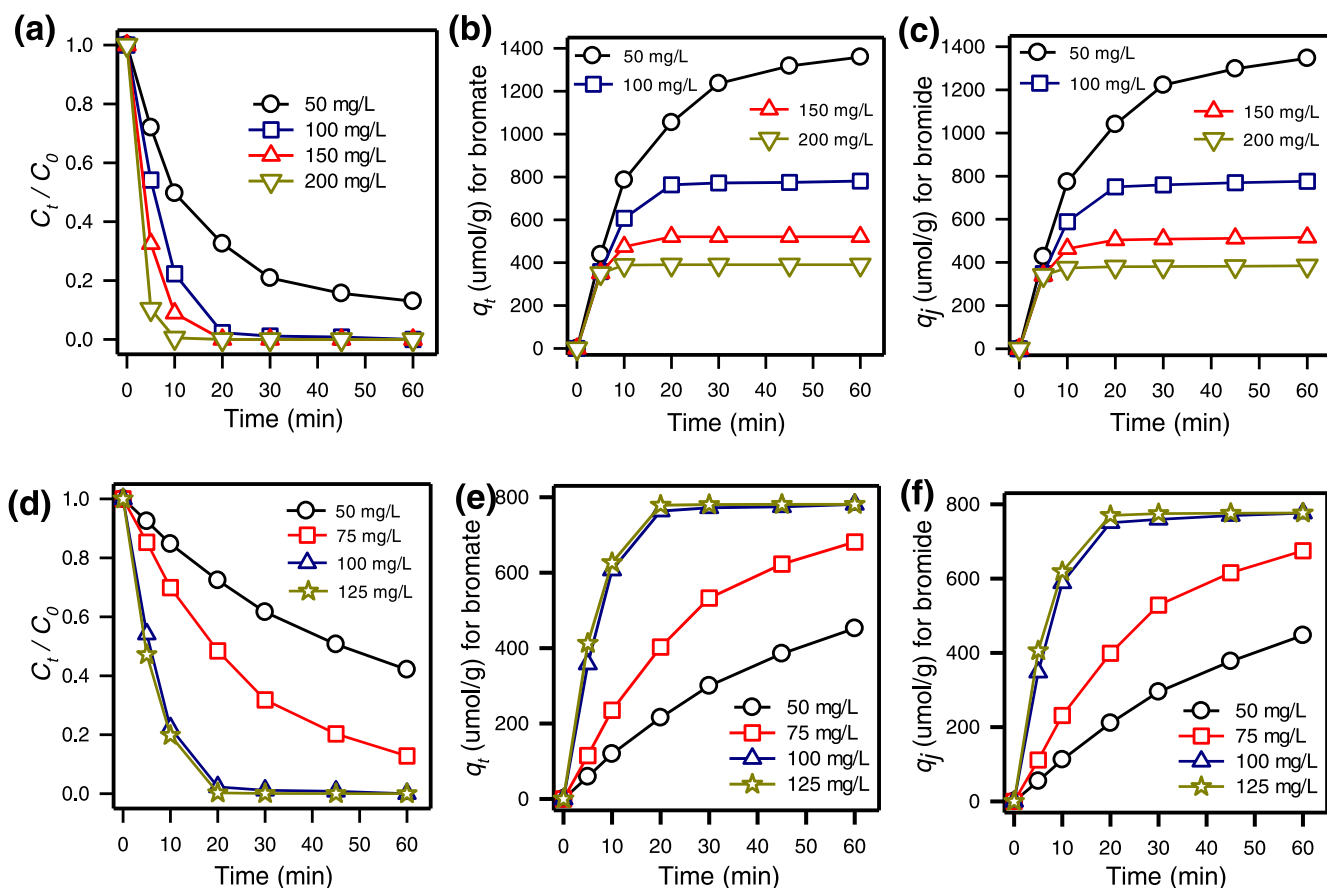


Fig. 7. Effect of catalyst (a–c) and NaBH₄ dosage (d–f) on bromate reduction using HPCO+NaBH₄ (HPCO = 100 mg/L, NaBH₄ = 100 mg/L, T = 30 °C).

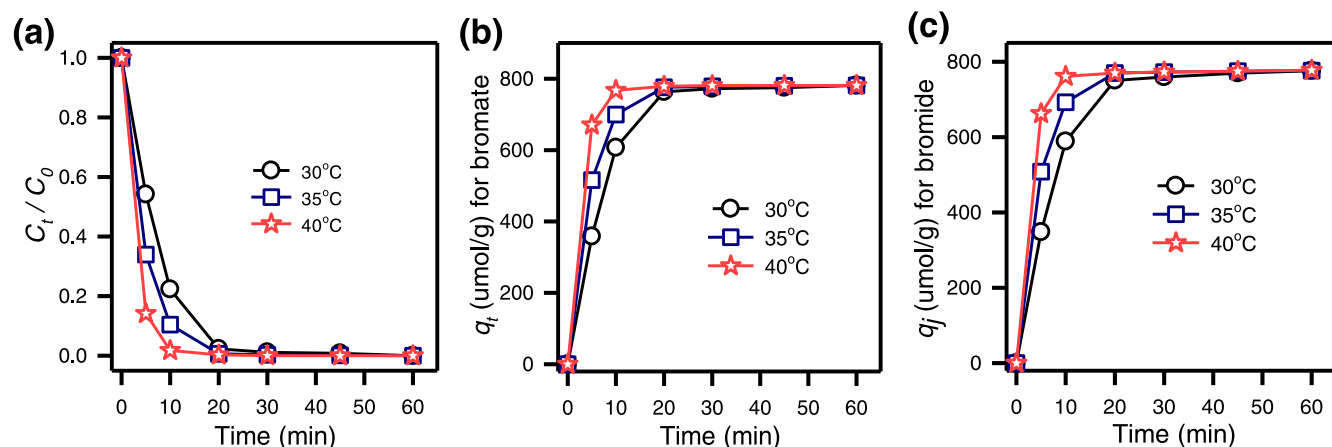


Fig. 8. Effect of temperatures on bromate reduction using HPCO+NaBH₄ (HPCO = 100 mg/L, NaBH₄ = 100 mg/L, T = 30 °C).

40 °C. This validates the enhancing effect of elevated temperatures on bromate reduction using HPCO/NaBH₄ system. Besides, bromate removal kinetics at various temperatures were further calculated via the pseudo first order rate law as the following equation (Eq. (5)):

$$C_t = C_0 \exp(-k_{obs}t) \quad (5)$$

where k_{obs} (min^{-1}) represents the observed rate constant of the pseudo first order equation. At 30 °C, bromate reduction kinetics was calculated as 0.148 min^{-1} (Table S2), which was significant increased to 0.1758 min^{-1} and 0.213 min^{-1} at 35 °C and 40 °C, respectively, asserting the effectiveness of elevated temperatures to bromate

reduction kinetics using HPCO catalyzed NaBH₄. Additionally, as k_{obs} was increased along with higher temperatures, the relationship between k_{obs} and temperatures was further correlated via the Arrhenius equation as follows (Eq. (6)):

$$\ln k_{obs} = \ln A - E_a/RT \quad (6)$$

where A represents the pre-exponential factor (min^{-1}); R is the gas constant (J/K mol); T is temperature of solution in Kelvin (K); E_a is the activation energy (kJ/mol). A plot (Fig. S7) indicated the correlation of $\ln k_{obs}$ versus $1/T$, indicating that the data points were well-fitting by linear regression ($R^2 = 0.997$), then E_a was calculated as 28.5 kJ/mol.

For comparisons, E_a values of the reported studies for bromate reduction were also summarized and listed in Table S3; and E_a of HPCO was considerably lower than many reported values by different catalysts, including precious metal catalysts. This result confirms that HPCO is a robust and competitive heterogeneous catalyst for bromate reduction.

On the other hand, bromate removal efficiencies and bromide generation capacities were also presented in Fig. 8(b) and (c), respectively. One can be noted that the bromate removal efficiencies could be reached to the equilibrium faster as the increase of temperature. In particular, while bromate removal efficiency afforded to equilibrium state in 20 min at 30 °C, it was even in a shorter time at higher temperatures (Fig. 8(b)). Besides, bromide generation capacities were also illustrated as shown in Fig. 8(c), indicating that bromide was also quickly produced when temperatures raised, which were corresponded to bromate reduction efficiencies. These results certainly certified the advantageous of elevated temperatures to bromate reduction using HPCO catalyzed NaBH₄.

3.5. Effect of initial pH of bromate solution

Since bromate reduction was performed using water batch experiments, pH of the solution is another crucial parameter affecting bromate reduction efficiency. Thus, the effect of different pH was further evaluated by adjusting the initial pH of bromate solution from 3 to 11. Fig. 9 (a) presents bromate reduction efficiency at various pH; and it can be noted that bromate reduction was slightly accelerated at lower pH of acidic conditions (i.e., pH = 3, 5) whereas bromate reduction was certainly influenced at higher pH of basic conditions (i.e., pH = 9, 11). In particular, at neutral condition of pH = 7, bromate was totally reduced within 20 min. When pH was lightly lowered as pH = 5, bromate was reduced faster, which could be even much faster at strongly acidic condition of pH = 3. In contrast, bromate was slowly reduced at slightly basic condition of pH = 9 whereas it was even much influenced at strongly basic condition of pH = 11. This demonstrates that bromate reduction was favorable in acidic conditions while higher pH of basic conditions seemed to be adverse for bromate reduction using HPCO catalyzed NaBH₄. The surface charges of HPCO were more positive at acidic conditions (as shown in zeta potentials analysis). Thus, anionic bromate ions were more attracted via electrostatic attraction force to the positive surface of HPCO where NaBH₄ was catalyzed to produce H₂ gas, thereby reducing bromate quickly [53]. Nevertheless, bromate reduction efficiencies were certainly decreased in basic conditions due to electrostatic repulsion between anionic bromate ions and more-negatively surface charges of HPCO, then leading to inefficient bromate reduction [53]. Moreover, bromate reduction efficiencies and bromide generation capacities at various pH values were also

determined as displayed in Fig. 9(b) and (c), respectively. And one can be seen that lower pH was more beneficial for bromate reduction efficiencies and bromide generation capacities while higher pH was certainly unfavorable. However, bromate removal efficiencies and bromide generation capacities were still comparable at various pH values by using HPCO+NaBH₄ system.

3.6. Effect of co-existing anions on bromate reduction

Since bromate is usually found in water where consisted of many ions, especially anions, it is necessary to investigate the effect of co-existing anions (i.e., nitrate, sulfate, phosphate) to bromate reduction using HPCO catalyzed NaBH₄. Before evaluating the effect of different anions, bromate solution containing equivalent concentration (i.e., 10 mg/L) of those co-existing anions was firstly prepared. As shown in Fig. 10(a), bromate reduction was slightly slower in the presence of co-existing anions. However, 100% of bromate removal was still afforded after 60 min, revealing the superior catalytic activities of HPCO catalyzed NaBH₄ for bromate reduction, even in a complex matrix of various anions. Besides, the generation of bromide converted from bromate reduction was also necessarily quantified; and there was no significant difference of bromide generation with or without co-existing anions (Fig. 10(b)), proving that HPCO+NaBH₄ was still capable to reduce bromate to bromide in the presence of those competing anions. Interestingly, while the concentration of phosphate and sulfate were unchanged by HPCO catalyzed NaBH₄, a small amount of nitrate was certainly removed after 60 min as C_t/C_0 was 0.77. This result implies that HPCO+NaBH₄ could also remove/reduce nitrate in water to produce nitrite, which is also reported in previous literature [11].

3.7. Recyclability of HPCO

Since HPCO showed superior catalytic activities for catalyzing NaBH₄ to reduce bromate in water, it is crucial to investigate the reusability of HPCO for continuous bromate reduction. As shown in Fig. 10 (c), bromate removal efficiencies were almost unchanged as almost 100% bromate removal was still afforded while the generation of bromide was also remained after five-consecutive cycles. Fig. 10(d) reveals that the spent HPCO showed a very comparable XRD pattern to that of original HPCO without significant variations, indicating the high stability of HPCO over the multiple-cycle application. This result confirms that HPCO was highly reusable with outstanding-stable catalytic activities reduce bromate to bromide in water, even without any regeneration treatment.

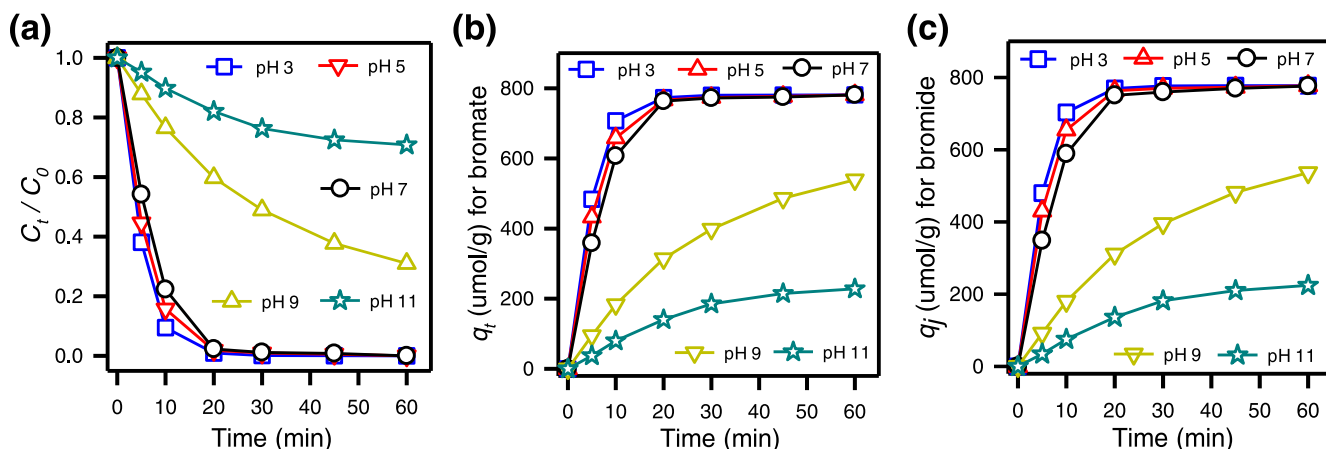


Fig. 9. Effect of pH on bromate reduction using HPCO+NaBH₄ (HPCO = 100 mg/L, NaBH₄ = 100 mg/L, T = 30 °C).

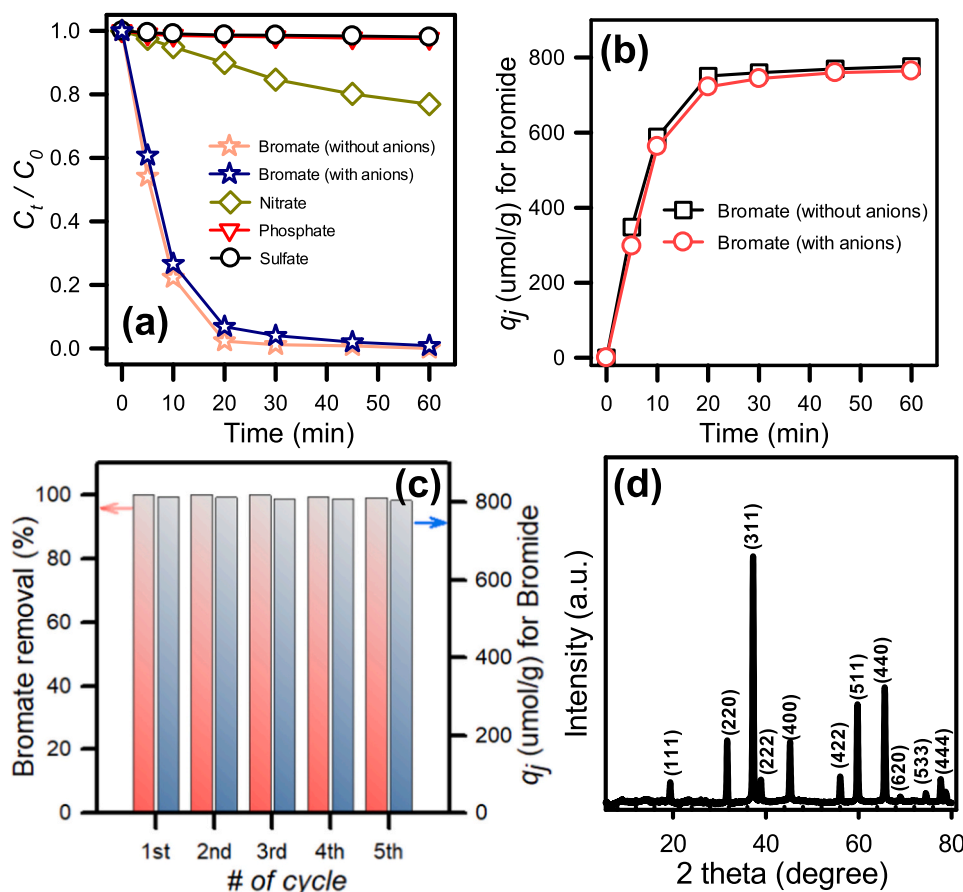


Fig. 10. Effect of co-existing anions on bromate reduction using HPCO+NaBH₄ (a) removal efficiency for bromate, and (b) conversion efficiency for bromide; (c) recyclability test of HPCO for bromate reduction (HPCO = 100 mg/L, NaBH₄ = 100 mg/L, T = 30 °C), and (d) XRD pattern of used HPCO.

4. Conclusion

In this study, a 2D hexagonal porous Co₃O₄ (HPCO) was successfully fabricated via one-step calcination of a coordinated framework CoTMC. The resulting HPCO not only retained the original 2D hexagonal morphology of the pristine CoTMC, but also comprised of many pores and Co₃O₄ NP distributing evenly over the surface. More importantly, this HPCO exhibited remarkable surficial oxygen vacancies as well as textural properties in comparison with the commercial Co₃O₄ NP. These significant characteristics of HPCO contributed to its outstanding catalytic activities for catalyzing NaBH₄ to reduce bromate in water. Moreover, HPCO also exhibited a low E_a of 28.5 kJ/mol for bromate reduction, which is lower than the reported values by many catalysts, especially noble metal catalysts. HPCO could also retain its high catalytic activities for bromate reduction and bromide generation over multiple-cycles, making it an outstanding and promising heterogeneous catalyst for bromate reduction via catalytic hydrogenation in water.

CRedit authorship contribution statement

Duong Dinh Tuan: Conceptualization, Methodology, Data curation. **Hongta Yang:** Data curation. **Nguyen Nhat Huy:** Visualization, Investigation. **Eilhann Kwon:** Supervision. **Ta Cong Khiem:** Validation. **Siming You:** Supervision. **Jechan Lee:** Writing - review & editing. **Kun-Yi Andrew Lin:** Writing - review & editing.

Declaration of Competing Interest

The authors declare that they have no known competing financial interests or personal relationships that could have appeared to influence

the work reported in this paper.

Acknowledgements

This work is supported by the Ministry of Science and Technology (MOST) (110-2636-E-005-003-), Taiwan, and financially supported by the “Innovation and Development Center of Sustainable Agriculture” from The Featured Areas Research Center Program within the framework of the Higher Education Sprout Project by the Ministry of Education (MOE), Taiwan. The authors gratefully acknowledge the use of SQUID000200 of MOST110-2731-M-006-001 belonging to the Core Facility Center of National Cheng Kung University.

Appendix A. Supporting information

Supplementary data associated with this article can be found in the online version at [doi:10.1016/j.jece.2021.105809](https://doi.org/10.1016/j.jece.2021.105809).

References

- [1] F. Soltermann, C. Abegglen, C. Götz, U. von Gunten, Bromide sources and loads in Swiss surface waters and their relevance for bromate formation during wastewater ozonation, *Environ. Sci. Technol.* 50 (18) (2016) 9825–9834.
- [2] R.J. Garcia-Villanova, M.V. Oliveira Dantas Leite, J.M. Hernández Hierro, S. de Castro Alfageme, C. García Hernández, Occurrence of bromate, chlorite and chlorate in drinking waters disinfected with hypochlorite reagents. Tracing their origins, *Sci. Total Environ.* 408 (12) (2010) 2616–2620.
- [3] U. Pinkernell, U. von Gunten, Bromate minimization during ozonation: mechanistic considerations, *Environ. Sci. Technol.* 35 (12) (2001) 2525–2531.
- [4] U. von Gunten, J. Hoigne, Bromate formation during ozonation of bromide-containing waters: interaction of ozone and hydroxyl radical reactions, *Environ. Sci. Technol.* 28 (7) (1994) 1234–1242.

- [5] K. Liu, J.H. Lu, Y.F. Ji, Formation of brominated disinfection by-products and bromate in cobalt catalyzed peroxymonosulfate oxidation of phenol, *Water Res.* 84 (2015) 1–7.
- [6] K.Y.A. Lin, S.Y. Chen, Catalytic reduction of bromate using ZIF-derived nanoscale cobalt/carbon cages in the presence of sodium borohydride, *ACS Sustain. Chem. Eng.* 3 (12) (2015) 3096–3103.
- [7] K. Listiarini, J.T. Tor, D.D. Sun, J.O. Leckie, Hybrid coagulation-nanofiltration membrane for removal of bromate and humic acid in water, *J. Membr. Sci.* 365 (1–2) (2010) 154–159.
- [8] A. Bhatnagar, Y. Choi, Y. Yoon, Y. Shin, B.H. Jeon, J.W. Kang, Bromate removal from water by granular ferric hydroxide (GFH), *J. Hazard. Mater.* 170 (1) (2009) 134–140.
- [9] Y. Zhong, Q. Yang, G. Fu, Y. Xu, Y. Cheng, C. Chen, R. Xiang, T. Wen, X. Li, G. Zeng, Denitrifying microbial community with the ability to bromate reduction in a rotating biofilm-electrode reactor, *J. Hazard. Mater.* 342 (2018) 150–157.
- [10] H. Chen, Z. Xu, H. Wan, J. Zheng, D. Yin, S. Zheng, Aqueous bromate reduction by catalytic hydrogenation over Pd/Al₂O₃ catalysts, *Appl. Catal. B-Environ.* 96 (3–4) (2010) 307–313.
- [11] K.-Y.A. Lin, H.-A. Chang, R.-C. Chen, MOF-derived magnetic carbonaceous nanocomposite as a heterogeneous catalyst to activate oxone for decolorization of Rhodamine B in water, *Chemosphere* 130 (2015) 66–72.
- [12] J. Restivo, O.S.G.P. Soares, J.J.M. Órfão, M.F.R. Pereira, Metal assessment for the catalytic reduction of bromate in water under hydrogen, *Chem. Eng. J.* 263 (2015) 119–126.
- [13] K.Y.A. Lin, C.H. Lin, S.Y. Chen, H. Yang, Enhanced photocatalytic reduction of concentrated bromate in the presence of alcohols, *Chem. Eng. J.* 303 (2016) 596–603.
- [14] Y.T. Chiu, H. Wang, J. Lee, K.Y.A. Lin, Reductive and adsorptive elimination of bromate from water using Ru/C, Pt/C and Pd/C in the absence of H₂: a comparative study, *Process Saf. Environ. Prot.* 127 (2019) 36–44.
- [15] Y.T. Chiu, P.Y. Lee, T. Wi-Afedzi, J. Lee, K.A. Lin, Elimination of bromate from water using aluminum beverage cans via catalytic reduction and adsorption, *J. Colloid Interface Sci.* 532 (2018) 416–425.
- [16] Y. Marco, E. García-Bordeje, C. Franch, A.E. Palomares, T. Yuranova, L. Kiwi-Minsker, Bromate catalytic reduction in continuous mode using metal catalysts supported on monoliths coated with carbon nanofibers, *Chem. Eng. J.* 230 (2013) 605–611.
- [17] R. Peña-Alonso, A. Sicurelli, E. Callone, G. Carturan, R. Raj, A picoscale catalyst for hydrogen generation from NaBH₄ for fuel cells, *J. Power Sources* 165 (1) (2007) 315–323.
- [18] Y. Wei, W. Meng, Y. Wang, Y. Gao, K. Qi, K. Zhang, Fast hydrogen generation from NaBH₄ hydrolysis catalyzed by nanostructured Co-Ni-B catalysts, *Int. J. Hydrog. Energy* 42 (9) (2017) 6072–6079.
- [19] F. Li, Q. Li, H. Kim, CoB/open-CNTs catalysts for hydrogen generation from alkaline NaBH₄ solution, *Chem. Eng. J.* 210 (2012) 316–324.
- [20] B.H. Liu, Z.P. Li, A review: hydrogen generation from borohydride hydrolysis reaction, *J. Power Sources* 187 (2) (2009) 527–534.
- [21] N. Nurlan, A. Akmanova, S. Han, W. Lee, Enhanced reduction of aqueous bromate by catalytic hydrogenation using the Ni-based metal-organic framework Ni(4,4'-bipy)(1,3,5-BTC) with NaBH₄, *Chem. Eng. J.* 414 (2021), 128860.
- [22] K.Y.A. Lin, S.Y. Chen, Bromate reduction in water by catalytic hydrogenation using metal-organic frameworks and sodium borohydride, *RSC Adv.* 5 (54) (2015) 43885–43896.
- [23] A.E. Palomares, C. Franch, T. Yuranova, L. Kiwi-Minsker, E. García-Bordeje, S. Derrouiche, The use of Pd catalysts on carbon-based structured materials for the catalytic hydrogenation of bromates in different types of water, *Appl. Catal. B-Environ.* 146 (2014) 186–191.
- [24] J. Restivo, O.S.G.P. Soares, J.J.M. Órfão, M.F.R. Pereira, Bimetallic activated carbon supported catalysts for the hydrogen reduction of bromate in water, *Catal. Today* 249 (2015) 213–219.
- [25] Y. Chen, W. Yang, S. Gao, Y. Gao, C. Sun, Q. Li, Catalytic reduction of aqueous bromate by a non-noble metal catalyst of CoS₂ hollow spheres in drinking water at room temperature, *Sep. Purif. Technol.* 251 (2020), 117353.
- [26] Z. Wu, Y. Tang, X. Yuan, Z. Qiang, Reduction of bromate by zero valent iron (ZVI) enhances formation of brominated disinfection by-products during chlorination, *Chemosphere* 268 (2021), 129340.
- [27] K.Y.A. Lin, C.H. Lin, J.Y. Lin, Efficient reductive elimination of bromate in water using zero-valent zinc prepared by acid-washing treatments, *J. Colloid Interface Sci.* 504 (2017) 397–403.
- [28] D.D. Tuan, K.Y.A. Lin, ZIF-67-derived Co₃O₄ rhombic dodecahedron as an efficient non-noble-metal catalyst for hydrogen generation from borohydride hydrolysis, *J. Taiwan Inst. Chem. Eng.* 91 (2018) 274–280.
- [29] D.D. Tuan, C. Hung, W. Da Oh, F. Ghanbari, J.Y. Lin, K.A. Lin, Porous hexagonal nanoplate cobalt oxide derived from a coordination polymer as an effective catalyst for activating oxone in water, *Chemosphere* 261 (2020), 127552.
- [30] M. Zhang, X. Su, L. Ma, A. Khan, L. Wang, J. Wang, A.S. Maloletnev, C. Yang, Promotion effects of halloysite nanotubes on catalytic activity of Co₃O₄ nanoparticles toward reduction of 4-nitrophenol and organic dyes, *J. Hazard. Mater.* 403 (2021), 123870.
- [31] L. Su, K. Li, H. Zhang, M. Fan, D. Ying, T. Sun, Y. Wang, J. Jia, Electrochemical nitrate reduction by using a novel Co₃O₄/Ti cathode, *Water Res.* 120 (2017) 1–11.
- [32] A. Al Nafey, A. Addad, B. Sieber, G. Chastanet, A. Barras, S. Szunerits, R. Boukherroub, Reduced graphene oxide decorated with Co₃O₄ nanoparticles (rGO-Co₃O₄) nanocomposite: a reusable catalyst for highly efficient reduction of 4-nitrophenol, and Cr(VI) and dye removal from aqueous solutions, *Chem. Eng. J.* 322 (2017) 375–384.
- [33] A.A. Keller, H. Wang, D. Zhou, H.S. Lenihan, G. Cherr, B.J. Cardinale, R. Miller, Z. Ji, Stability and aggregation of metal oxide nanoparticles in natural aqueous matrices, *Environ. Sci. Technol.* 44 (6) (2010) 1962–1967.
- [34] C.P. Tso, C.M. Zhung, Y.H. Shih, Y.M. Tseng, S.C. Wu, R.A. Doong, Stability of metal oxide nanoparticles in aqueous solutions, *Water Sci. Technol.* 61 (1) (2010) 127–133.
- [35] J. Zhu, R. Li, W. Niu, Y. Wu, X. Gou, Fast hydrogen generation from NaBH₄ hydrolysis catalyzed by carbon aerogels supported cobalt nanoparticles, *Int. J. Hydrog. Energy* 38 (25) (2013) 10864–10870.
- [36] Y.C. Tsai, N.N. Huy, D. Tsang, K.A. Lin, Metal organic framework-derived 3D nanostructured cobalt oxide as an effective catalyst for soot oxidation, *J. Colloid Interface Sci.* 561 (2020) 83–92.
- [37] M.C. Li, D. Ding, K.Y.A. Lin, E. Kwon, Cobalt-based coordination polymers as heterogeneous catalysts for activating Oxone to degrade organic contaminants in water: a comparative study, *Sep. Purif. Technol.* 236 (2020), 116245.
- [38] T.J. Niiranen, E.L. McCabe, M.G. Larson, M. Henglin, N.K. Lakdawala, R.S. Vasan, S. Cheng, O-2(2-)/O- functionalized oxygen-deficient Co₃O₄ nanorods as high performance supercapacitor electrodes and electrocatalysts towards water splitting, *Nano Energy* 38 (2017) 155–166.
- [39] D.W. Wang, Q.H. Wang, T.M. Wang, Morphology-controllable synthesis of cobalt oxalates and their conversion to mesoporous Co₃O₄ nanostructures for application in supercapacitors, *Inorg. Chem.* 50 (14) (2011) 6482–6492.
- [40] M. Herrero, P. Benito, F. Labajos, V. Rives, Nanosize cobalt oxide-containing catalysts obtained through microwave-assisted methods, *Catal. Today* 128 (3) (2007) 129–137.
- [41] V.K. Patel, J.R. Saurav, K. Gangopadhyay, S. Gangopadhyay, S. Bhattacharya, Combustion characterization and modeling of novel nanoenergetic composites of Co₃O₄/nAl, *RSC Adv.* 5 (28) (2015) 21471–21479.
- [42] Q. Liu, L.C. Wang, M. Chen, Y. Cao, H.Y. He, K.N. Fan, Dry citrate-precursor synthesized nanocrystalline cobalt oxide as highly active catalyst for total oxidation of propane, *J. Catal.* 263 (1) (2009) 104–113.
- [43] X. Sui, N. Kong, X. Wang, Y. Fang, X. Hu, Y. Xu, W. Chen, K. Wang, D. Li, W. Jin, F. Lou, Y. Zheng, H. Hu, L. Gong, X. Zhou, H. Pan, W. Han, Promoting effects of In₂O₃ on Co₃O₄ for CO oxidation: tuning O-2 activation and CO adsorption strength simultaneously, *ACS Catal.* 4 (11) (2014) 4143–4152.
- [44] L. Li, J. Yan, T. Wang, Z.J. Zhao, J. Zhang, J. Gong, N. Guan, Sub-10 nm rutile titanium dioxide nanoparticles for efficient visible-light-driven photocatalytic hydrogen production, *Nat. Commun.* 6 (2015), 5881.
- [45] A. Naldoni, M. Allieta, S. Santangelo, M. Marelli, F. Fabbri, S. Cappelli, C. L. Bianchi, R. Psaro, V. Dal Santo, Effect of nature and location of defects on bandgap narrowing in black TiO₂ nanoparticles, *J. Am. Chem. Soc.* 134 (18) (2012) 7600–7603.
- [46] Z. Wang, W. Wang, L. Zhang, D. Jiang, Surface oxygen vacancies on Co₃O₄ mediated catalytic formaldehyde oxidation at room temperature, *Catal. Sci. Technol.* 6 (11) (2016) 3845–3853.
- [47] L.L. Feng, M. Fan, Y. Wu, Y. Liu, G.D. Li, H. Chen, W. Chen, D. Wang, X. Zou, Metallic Co₉S₈ nanosheets grown on carbon cloth as efficient binder-free electrocatalysts for the hydrogen evolution reaction in neutral media, *J. Mater. Chem. A* 4 (18) (2016) 6860–6867.
- [48] L. Liu, Z. Jiang, L. Fang, H. Xu, H. Zhang, X. Gu, Y. Wang, Probing the crystal plane effect of Co₃O₄ for enhanced electrocatalytic performance toward efficient overall water splitting, *ACS Appl. Mater. Interfaces* 9 (33) (2017) 27736–27744.
- [49] C. Wu, F. Wu, Y. Bai, B. Yi, H. Zhang, Cobalt boride catalysts for hydrogen generation from alkaline NaBH₄ solution, *Mater. Lett.* 59 (14–15) (2005) 1748–1751.
- [50] R. Krishna, D.M. Fernandes, C. Dias, J. Ventura, E. Venkata Ramana, C. Freire, E. Titus, Novel synthesis of Ag@Co/RGO nanocomposite and its high catalytic activity towards hydrogenation of 4-nitrophenol to 4-aminophenol, *Int. J. Hydrog. Energy* 40 (14) (2015) 4996–5005.
- [51] R.P. Pandey, K. Rasool, P. Abdul Rasheed, K.A. Mahmoud, Reductive sequestration of toxic bromate from drinking water using Lamellar two-dimensional Ti₃C₂TX (MXene), *ACS Sustain. Chem. Eng.* 6 (6) (2018) 7910–7917.
- [52] A. Zeino, A. Abulkibash, M. Khaled, M. Atieh, Bromate removal from water using doped iron nanoparticles on multiwalled carbon nanotubes (CNTs), *J. Nanomater.* 2014 (2014) 1–9.
- [53] X. Wu, Q. Yang, D. Xu, Y. Zhong, K. Luo, X. Li, H. Chen, G. Zeng, Simultaneous adsorption/reduction of bromate by nanoscale zerovalent iron supported on modified activated carbon, *Ind. Eng. Chem. Res.* 52 (35) (2013) 12574–12581.